The effective self-diffusion coefficient of solvent molecules in colloidal crystals

ARTICLE *in* JOURNAL OF COLLOID AND INTERFACE SCIENCE · FEBRUARY 1991

Impact Factor: 3.37 · DOI: 10.1016/0021-9797(91)90332-3

The Effective Self-Diffusion Coefficient of Solvent Molecules in Colloidal Crystals

P. VENEMA,[1] R. P. W. J. STRUIS,* J. C. LEYTE, AND D. BEDEAUX

*Department of Physical and Macromolecular Chemistry, Gorlaeus Laboratories, P.O. Box 9502, 2300 RA Leiden, The Netherlands; and *Institut für Physikalische Chemie, Universität Basel, Klingelbergstrasse 80, CH-4056 Basel, Switzerland*

Received March 12, 1990; accepted June 8, 1990

An analysis is given of the self-diffusion of solvent molecules in a colloidal crystal. The effective self-diffusion coefficient of the solvent molecules is calculated, by solving the Laplace equation, as a function of the volume fraction of the colloidal particles. Using an expansion of the probability distribution for a given solvent molecule in terms of solid spherical harmonics it is possible to obtain the exact value for the effective self-diffusion coefficient for all volume fractions up to dense packing. It is found that, contrary to earlier predictions (1–3), the self-diffusion coefficient changes from a convex decreasing function to a concave decreasing function of the volume fraction at a volume fraction about 50% of close packing. Experimental results obtained using the 1-H NMR pulsed field gradient technique are also discussed in this paper and confirm the change from convex to concave behavior

1. INTRODUCTION

The behavior of the self-diffusion coefficient of small solvent molecules in colloidal systems has been studied extensively. Due to the presence of the colloidal particles the value of the self-diffusion coefficient of the solvent molecules is modified and in general decreases toward a lower value compared to the value of the self-diffusion coefficient in the pure solvent. It is convenient to describe this effect in terms of an effective self-diffusion coefficient. Such an effective transport coefficient may be derived by averaging over volumes that are large compared to the characteristic dimensions of the inhomogeneities of the system but that are small compared to the overall size of the system. The decrease of the effective self-diffusion coefficient may be attributed to two mechanisms. The first mechanism, often referred to as the obstruction effect, is that a colloidal particle excludes a certain fraction of the total volume from a diffusing solvent molecule, so that this molecule is hindered in its diffusional motion which leads to a decrease of the effective self-diffusion coefficient. The second mechanism is related to the molecular interaction between solvent molecules and the colloidal particles which may lead to a further decrease of the effective self-diffusion coefficient. These two mechanisms have already been discussed by Wang (1), who has derived an expression for the effective diffusion coefficient of the solvent molecules as a function of the volume fraction of identical spheroidal colloidal particles. For the obstruction effect Wang derives the formula $D_{\text{eff}} = D_0(1 - \frac{3}{2}\phi)$; here D_{eff} is the effective value of the self-diffusion coefficient of the solvent molecules, D_0 being the self-diffusion coefficient in the pure solvent and ϕ being the volume fraction of spherical colloidal particles. This expression was later corrected by Bell (2) in his study of the diffusion of ions in electrical fields to $D_{\text{eff}} = D_0(1 - \frac{1}{2}\phi)$. These expressions were obtained by solving essentially single sphere problems and are therefore expected to be valid only at moderate volume fractions. In a

[1] To whom correspondence should be addressed.

0021-9797/91 $3.00

more recent paper by Jönsson *et al.* (3) another expression for the effective diffusion coefficient is derived. Using a cell model and arguments from the thermodynamics of irreversible processes they obtain $D_{\text{eff}} = D_0(1 + \frac{1}{2}\phi)^{-1}$. They express the hope that their formula will be valid over the full range of volume fractions of the colloidal particles. Their measurements of the effective self-diffusion coefficient D_{eff} of water molecules in a polymethyl methacrylate latex systematically fall below the curve given by their formula. They express the opinion that this deviation is more likely an effect of swelling and of a direct interaction between the water molecules and the polymer segments on the particle surface rather than an effect of the approximations in their model. In order to support this conclusion they performed Monte Carlo simulations up to $\phi \cong 0.5$, where a test particle is performing a random walk on a face centered cubic lattice of obstructing spheres. They find that the Monte Carlo results, up to $\phi \cong 0.5$, coincide with their theoretical formula. In our exact evaluation of the effective self-diffusion coefficient of a particle in a face centered cubic lattice of obstructing spheres we find that up to $\phi \cong 0.5$ their expression is indeed in good approximation correct. For larger volume fractions, however, the exact value falls significantly below the values given by their formula. For these larger volume fractions the approximations in their model are clearly no longer justified (cf. Fig. 1). We will return to this point in Section 4.

In order to obtain a greater insight into the behavior of the effective self-diffusion coefficient, especially at high volume fractions, we will focus in the theoretical part of this paper, Sections 2–4, on the obstruction effect, and neglect all other interactions between the solvent molecule and the colloidal particles. We will consider a so-called colloidal crystal, in which the (spherical) colloidal particles are fixed with their centers on the lattice points of a regular array. The position and time dependent (unnormalized) probability distribution of the diffusing solvent particle $n(\mathbf{r}, t)$ satisfies the equation

$$\frac{\partial}{\partial t} n(\mathbf{r}, t) = -\text{div}\, \mathbf{j}(\mathbf{r}, t), \qquad [1.1]$$

where $\mathbf{j}(\mathbf{r}, t)$ is the diffusion current which is given by Fick's law

$$\mathbf{j}(\mathbf{r}, t) = -D_0 \text{grad}\, n(\mathbf{r}, t). \qquad [1.2]$$

Both the equations above are valid outside the colloidal particles. Inside the colloidal particles both $n(\mathbf{r}, t)$ and $\mathbf{j}(\mathbf{r}, t)$ are zero. On the surface of the colloidal particles the normal component of the diffusion current must be continuous and consequently one must solve the above equations with a boundary condition that the normal component of the diffusion current on the surface of the colloidal particles is zero.

In Section 2 we solve the above equations explicitly for the special case in which a stationary diffusional flow is caused by applying an externally controlled gradient $\mathbf{G}$ in the probability density, using the lattice symmetry. In this solution $n(\mathbf{r})$ is written as a superposition of $\mathbf{G} \cdot \mathbf{r}$ and a field which is caused by an imaginary source-sink distribution inside the colloidal particles. This imaginary source-sink distribution is chosen in such a way that the boundary condition at the surface of the spherical colloidal particles is fulfilled and is given in terms of its multipole moments. An effective self-diffusion coefficient may be defined by averaging Eq. (1.1) over a volume which is large compared to the lattice spacing but which is small compared to the overall size of the system. In view of the lattice symmetry this is equivalent to simply averaging over the Wigner–Seitz cell. Using the solution for $n(\mathbf{r})$ given in Section 2 the averaging over the Wigner–Seitz cell is performed in Section 3. Using the results we subsequently derive in Section 4 the following general expression for the effective self-diffusion coefficient

$$D_{\text{eff}} = D_0 \frac{1}{(1 - \phi)} \frac{(1 - 2K\phi)}{(1 + K\phi)}, \qquad [1.3]$$

where the ϕ dependent coefficient K is given

as an expansion in the cube root of ϕ by

$$K = \sum_i m_i(\phi/\phi_{max})^{i/3}. \quad [1.4]$$

Here ϕ_{max} is the volume fraction of the spheres at dense packing. The coefficients m_i are given explicitly in Section 4 up to $i = 24$ for the cubic lattices. The exact value of m_i is found by iteration by taking multipoles of the imaginary source-sink distribution into account up to a sufficiently high order. The advantage of this approach is that it yields exact values for the m_i's up to a certain order; the disadvantage is that many particle interactions between lower-order multipoles are neglected as they do not contribute to m_i up to that order. We find that close to dense packing, $\phi > 0.85\phi_{max}$, the convergence of the theoretical value is greatly improved if one uses a finite number of multipoles and solves the set of linear equations for these multipoles, which are given in Section 3, by direct inversion rather than by iteration. In this way many particle interactions between the finite number of multiples are taken into account to arbitrary order in $(\phi/\phi_{max})^{1/3}$. In Fig. 1 the results obtained by the method of direct inversion are plotted for the three cubic lattices. The reader whose main interest is the comparison of these results with the experimental data may skip the analytical details of the theoretical analysis in Sections 2–4 and move on to Section 5 after reading the introduction. Using the fact that $m_0 = \frac{1}{2}$ is independent of the choice of the lattice one finds, expanding the above expression in powers of the cubic root of ϕ,

$$D_{eff} = D_0(1 - 0.5\phi + 0.25\phi^2 - 0.125\phi^3 + 0.0625\phi^4 + O(\phi^{13/3})). \quad [1.5]$$

Expanding the expression given in Ref. (3) gives the same result up to the fourth power in ϕ. We find that the higher-order terms in our expansion [1.5] contribute significantly for $\phi \geqslant 0.5\phi_{max}$ and as a consequence our result leads to values of the effective self-diffusion coefficient which decrease strongly if one approaches ϕ_{max}. This behavior differs not only quantitatively but also qualitatively from the formula given in Ref. (3) in the sense that the functional dependence changes from convex to concave for increasing volume fractions. This qualitative behavior is in agreement with our experimental results for the diffusion of water molecules through a latex suspension which are discussed in Section 5. In order to obtain also quantitative agreement it is necessary to introduce an effective volume fraction.

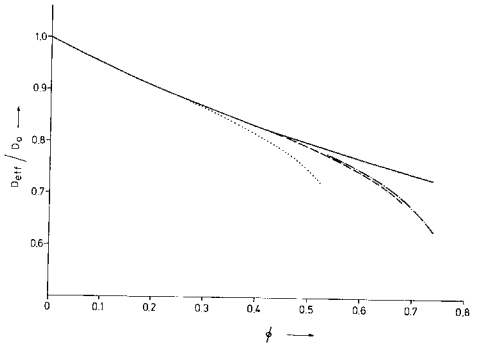

FIG. 1. Plot of the effective self-diffusion coefficient D_{eff}/D_0 as a function of the volume fraction ϕ for the SC array (· · ·), the BCC array (---), and the FCC array (-·-·-) obtained by the method of direct inversion. The curve $(1 + 0.5\phi)^{-1}$ from Ref. (3) is denoted by the solid curve.

2. THEORY

The colloidal system is modeled as consisting of impenetrable, immobile, and spherical colloidal particles with a radius a placed with their centers on the lattice points of a regular array. We restrict ourselves to regular arrays of the cubic type (simple cubic, body centered cubic, or face centered cubic), because it seems well established nowadays (4, 5) that colloidal crystals occur in either a BCC or a FCC arrangement depending on ionic strength and volume fraction. The assumption of immobility is clearly satisfied in a colloidal crystal, because the colloidal particles are "bound" to lattice points in the array by electrostatic forces. The impenetrability of the colloidal particles is not an essential limitation in the calculation and may in principle be replaced by a different kind of boundary condition. In

fact one may make the spheres penetrable and use a diffusion coefficient inside the spheres. If this diffusion coefficient only depends on the distance to the center of the spheres it is not difficult to give the resulting expression for the effective diffusion coefficient similar to the one given above; see in this context, e.g., Ref (6). As the mobility of the solvent molecules in the system under consideration is small inside the colloidal particles compared to the value in the bulk we will simply set the diffusion coefficient inside the colloidal particles equal to zero and use the boundary condition that the normal component of the diffusion flow vanishes at the surface of the colloidal particles.

One finds that a stationary probability distribution satisfies the Laplace equation outside the colloidal particles if the diffusion current given in Eq. [1.2] is substituted in Eq. [1.1]:

$$\Delta n = 0. \qquad [2.1]$$

In order to establish a nonzero diffusional flow in the system we apply an externally controlled gradient $\mathbf{G}$ in the probability density. In principle the resulting diffusion flow may not only depend on the direction of $\mathbf{G}$ but its average may also have a direction which differs from the direction of $\mathbf{G}$. This then defines an effective diffusion tensor. It follows from the Onsager relations that this tensor is symmetric, which implies that it may be diagonalized with three diffusion coefficients which may in principle be different form each other in three mutually orthogonal directions. In view of the symmetry of the cubic arrays these three diffusion coefficients are all identical so that the diffusion tensor reduces to a scalar. This implies that we may choose the gradient $\mathbf{G}$, without loss of generality, along one of the major axes of the cubic arrays. In order to construct the general solution of Eq. [2.1] outside the colloidal spheres we introduce the as yet undetermined multipole moments $p_{l,m}$ of an imaginary source-sink distribution inside the spheres. These enable us to write the general solution outside the spheres in terms of solid spherical harmonics (as defined in Ref. (7)) as

$$n(\mathbf{r}) = n_0 + \sum_{\lambda} \sum_{l,m}{}' p_{l,m} \left(\frac{a}{r_\lambda}\right)^{l+1} Y_{l,m}(\theta_\lambda, \phi_\lambda) + \mathbf{G}\cdot\mathbf{r}, \qquad [2.2]$$

where $l = 0, 1, 2, 3, 4, \cdots$ and $m = -l, -l + 1, \cdots, 0, \cdots, l - 1, l$. Furthermore λ labels the lattice site $\mathbf{R}_\lambda$, while

$$\mathbf{r}_\lambda = \mathbf{r} - \mathbf{R}_\lambda \equiv r_\lambda(\sin\theta_\lambda\cos\phi_\lambda, \sin\theta_\lambda\sin\phi_\lambda, \cos\theta_\lambda). \qquad [2.3]$$

The prime in the summation sign indicates that the $l = 0$ term is excluded. We will use this convention also in the rest of the article. Note that the multipole moments $p_{l,m}$ are independent of λ because of the translational symmetry of the lattice. In order to determine the multipole moments $p_{l,m}$ we have to use the boundary condition of a vanishing normal component of the diffusion current on the surface of the colloidal particles. Because all colloidal particles are equivalent in the arrays it is enough to do this for one reference sphere which we will take to be located in the lattice point $\mathbf{R}_\lambda = 0$. In order to write our solution in a more convenient form for further analysis we rewrite Eq. [2.2] by using a generalized form of the addition theorem (see Appendix A), which enables us to expand the "negative" multipole fields originating from lattice points $\mathbf{R}_\lambda \neq 0$ in terms of "positive" multipole fields originating from the lattice point $\mathbf{R}_\lambda = 0$. Thus we arrive at the expression

$$n(\mathbf{r}) = n_0 + \sum_{l,m}{}' p_{l,m}\left(\frac{a}{r}\right)^{l+1} Y_{l,m}(\theta_0, \phi_0) + \sum_{l',m}{}' \sum_{l,m} r^{l'} p_{l',m'} \times \frac{a^{l'+1} H(lm|l'm') U_{l+l',m-m'}}{d^{l+l'+1}} \times Y_{l,m}(\theta_0, \phi_0) + \mathbf{G}\cdot\mathbf{r}, \qquad [2.4]$$

where $H(lm|l'm')$ and $U_{l,m}$ are defined by

$$H(lm|l'm') = (-1)^{l'+m}\left[\frac{2l'+1}{2l+1}\right]^{1/2} \times \left[\frac{(l+l'-m+m')!(l'+l+m-m')!}{(l+m)!(l-m)!(l'+m')!(l'-m')!}\right]^{1/2} \quad [2.5]$$

and

$$U_{l,m} = \left[\frac{4\pi}{2l+1}\right]^{1/2} d^{l+1} S_{l,m}. \quad [2.6]$$

Here d is the nearest neighbor distance in the lattice. The $S_{l,m}$ are the so-called lattice sums which are defined by (8):

$$S_{l,m} \equiv \sum_{\lambda}{}' \frac{Y_{l,m}(\theta_\lambda, \phi_\lambda)}{R_\lambda^{l+1}}. \quad [2.7]$$

For cubic arrays these sums are unequal to zero only for l is even and $m = 0$ or a four-fold. It should be noted that $S_{2,0} = 0$ and that it is not a conditional convergent lattice sum, which depends on the form of the sample, as claimed by some authors (9, 10). The reason (11) for this is that one should use the retarded propagator, which is most conveniently done by introducing a convergence factor $\exp(-\epsilon r)$ with ϵ an infinitesimally small positive number. This enables us to perform the dipole sum $S_{2,0}$ by summing over a sphere of volume V and taking $V \to \infty$. This sum vanishes for reasons of symmetry for the cubic lattices. Using now the boundary condition on the surface of the colloidal particles and using the orthogonality of the spherical harmonics $Y_{l,m}(\theta_0, \phi_0)$ one finds a linear equation from which one can solve the multipole moments $p_{l,m}$. We find the matrix equation for the multipole moments $p_{l,m}$ (with $l \neq 0$)

$$\sum_{l',m'}{}' \left(\delta_{l,l'}\delta_{m,m'} - \frac{l}{l+1}\left(\frac{a}{d}\right)^{l+l'+1} \times H(lm|l'm')\, U_{l+l',m'-m}\right) p_{l',m'} = \frac{1}{2}\left(\frac{4\pi}{3}\right)^{1/2} Ga\,\delta_{l,1}\,\delta_{m,0}. \quad [2.8]$$

We use two methods to find an approximate solution. In both methods only a finite number of multipoles are taken into account. In the first method we represent the formal solution of Eq. [2.8] by $\mathbf{p} = (\vec{\mathbf{I}} + \vec{\mathbf{M}})^{-1} \cdot \mathbf{c}$, where the definition of $\vec{\mathbf{M}}$ and $\mathbf{p}$ are obvious from Eq. [2.8], and develop this solution as $\mathbf{p} = (\vec{\mathbf{I}} - \vec{\mathbf{M}} + \vec{\mathbf{M}}^2 - \vec{\mathbf{M}}^3 + \cdots) \cdot \mathbf{c}$. As $\vec{\mathbf{M}}$ is analytic in a/d and is zero for $a/d = 0$, the expansion for $\mathbf{p}$ in powers of $\vec{\mathbf{M}}$ leads to an expansion for $\mathbf{p}$ in powers of a/d. This corresponds with an expansion of the multipole moments $p_{l,m}$ in powers of the cube root of the volume fraction ϕ of the sinks. The second method is to invert the matrix $(\vec{\mathbf{I}} + \vec{\mathbf{M}})$ exactly for a growing number of multipoles $p_{l,m}$ so that the matrix becomes larger and larger. This process is continued until the required convergence is achieved in the result. The advantage of the first method is that we obtain an exact analytical result up to a certain power in the cube root of the volume fraction. The disadvantage of this method is that the convergence of the result for volume fractions close to dense packing is unsatisfactory. This point has been discussed in detail in Ref. (6). The second method accounts for the interactions between the finite number of multipoles to all orders, giving the same results for smaller volume fractions and converging much faster for volume fractions close to dense packing. Before proceeding to calculate $p_{l,m}$ explicitly, using these methods, we will in the following section first derive an expression for the effective rate coefficient in terms of $p_{l,m}$. Equation [2.8] shows that only multipole moments $p_{l,m}$ with l uneven and $m = 0$ or a four-fold occur.

3. EXPRESSION FOR THE EFFECTIVE SELF-DIFFUSION COEFFICIENT

In order to obtain an expression for the effective self-diffusion coefficient D_{eff} in terms of the multipole moments, we average the diffusion current $\mathbf{j}$ and the solvent density function n over volumes which are large compared to the characteristic dimensions of the inhomogeneities in the system but small compared to the overall size of the system. However, since we are dealing with colloidal crystals

where the system may be thought to be built up from replicas of just one Wigner–Seitz cell (with a colloidal particle in its center) we may restrict the averaging to the volume of one Wigner–Seitz cell.

The effective diffusion coefficient is defined by the relation

$$\langle \mathbf{j} \rangle = -D_{\text{eff}} \nabla \langle n \rangle, \qquad [3.1]$$

where $\langle \mathbf{j} \rangle$ and $\langle n \rangle$ are defined as

$$\langle \mathbf{j} \rangle = \frac{1}{\Omega} \int_{\Omega} \mathbf{j}(\mathbf{r}) d\mathbf{r} = \frac{1}{\Omega} \int_{\Omega - B} \mathbf{j}(\mathbf{r}) d\mathbf{r} \qquad [3.2]$$

and

$$\langle n \rangle = \frac{1}{\Omega} \int_{\Omega} n(\mathbf{r}) d\mathbf{r} = \frac{1}{\Omega} \int_{\Omega - B} n(\mathbf{r}) d\mathbf{r}, \qquad [3.3]$$

where Ω denotes the volume of a Wigner–Seitz cell and where B is the region in space occupied by the spherical colloidal particle and extending until an infinitesimally small distance outside its surface. In the second equality in the above equations we used the fact that inside the particle both n and $\mathbf{j}$ are zero so that the above integrals may be restricted to the region outside the spheres. The explicit solution for n and as a consequence for $\mathbf{j}$ outside the spherical colloidal particle is given in Eq. [2.2].

We will now proceed to evaluate the integral in Eq. [3.2]. For this purpose it is convenient to define the analytic continuation n^* of n. Outside and on the colloidal particles n^* equals n and inside the colloidal particles n^* is defined also by Eq. [2.2]. Using Eq. [1.2] we find

$$\begin{aligned} \langle \mathbf{j} \rangle &= -\frac{D_0}{\Omega} \int_{\Omega - B} \nabla n d\mathbf{r} \\ &= -\frac{D_0}{\Omega} \left(\int_{\Omega} \nabla n^* d\mathbf{r} - \int_{B} \nabla n^* d\mathbf{r} \right) \\ &= -\frac{D_0}{\Omega} \left(\int_{\Omega} \nabla n^* d\mathbf{r} - \int_{S} \hat{n} n dS \right). \end{aligned} \qquad [3.4]$$

Here S is the surface of the particle and $\hat{n}$ is the outward normal on the surface. Substituting Eq. [2.5] for n in the integral over the surface and using the orthonormal properties of the spherical harmonics, we find

$$\begin{aligned} \langle j_z \rangle = -D_0 \Bigg(\langle \nabla_z n^* \rangle - \frac{a^2}{\Omega} \left(\frac{4\pi}{3} \right)^{1/2} \\ \times \left[p_{1,0} + \sum_{l',m'}{}' p_{l',m'} \left(\frac{a}{d} \right)^{l'+2} \right. \\ \left. \times H(10|l'm') U_{1+l',m'} + \left(\frac{4\pi}{3} \right)^{1/2} Ga \right] \Bigg). \end{aligned} \qquad [3.5]$$

Note that the averaged diffusion current along the x- and y-axis is zero, because we apply the externally applied density gradient along the z-axis. We may eliminate the summation in Eq. [3.5] by using the boundary condition Eq. [2.6], which leads directly to

$$\langle j_z \rangle = -D_0 \left[\langle \nabla_z n^* \rangle - 3 \frac{a^2}{\Omega} \left(\frac{4\pi}{3} \right)^{1/2} p_{1,0} \right]. \qquad [3.6]$$

Clearly the gradient of the periodic part of n^* does not contribute to the integral, so it may be tempting to think that only the externally applied gradient $\mathbf{G}$ survives. However, there is another contribution. As explained in Ref. (7, p. 140), the field due to a dipole contains a delta function. The dipole moment $\mathbf{p}$ in the notation of Ref. (7) is related to the multipole moment $p_{1,0}$ as

$$\mathbf{p} = -\left(\frac{4\pi}{3} \right)^{1/2} a^2 p_{1,0} \hat{z}. \qquad [3.7]$$

The delta function contribution to the field due to the dipole is therefore given by

$$\left(\frac{4\pi}{3} \right)^{1/2} a^2 p_{1,0} \delta(\mathbf{r}) \hat{z}. \qquad [3.8]$$

This delta function also contributes to the integral of the gradient of n^* and as a result we find the expression

$$\langle \nabla_z n^* \rangle = G + \frac{a^2}{\Omega} \left(\frac{4\pi}{3} \right)^{1/2} p_{1,0}. \qquad [3.9]$$

Note that this expression is equivalent to

the expression for the so-called internal field, i.e., the electric field effective in polarizing a particle in an electric medium, given by Lorentz (12) for the case of cubic crystals. This value for the internal field leads to the Clausius–Mossotti expression for the dielectric constant and the Lorentz–Lorenz expression for the refractive index. It follows from Eq. [3.9] that this expression for the internal field is obtained by averaging the total ∇n^*-field over a Wigner–Seitz cell.

Combining Eqs. [3.6] and [3.9] gives

$$\langle j_z \rangle = -D_0 \frac{1 - 2\phi p_{1,0}/aG(4\pi/3)^{1/2}}{1 + \phi p_{1,0}/aG(4\pi/3)^{1/2}} \times \langle \nabla_z n^* \rangle. \quad [3.10]$$

The problem is now to relate $\langle \nabla_z n^* \rangle$ to $\nabla_z \langle n \rangle$. It is clear by direct integration that $\langle \nabla_z n^* \rangle$ is equal to the difference of the average values of n at the upper and lower surface of the Wigner–Seitz cell in the direction of the applied gradient $\mathbf{G}$ divided by the nearest neighbor distance d. As there can be no diffusional flow along these surfaces n must be constant along these surfaces. In consequence $\langle \nabla_z n^* \rangle$ is equal to the difference of n between any pair of points on the upper and lower surface divided by d. Using the symmetry of the problem one may now conclude that if one takes a pair of points outside the colloidal particles in two adjoining cells which can be obtained from each other by translation over a lattice vector parallel to $\mathbf{G}$, the difference of n in these two points divided by d is equal to $\langle \nabla_z n^* \rangle$. From this fact and from the fact that n equals zero inside the spheres it now follows that the difference of $\langle n \rangle$ in two adjacent cells divided by d is equal to $(1 - \phi)\langle \nabla_z n^* \rangle$. Identifying the difference of $\langle n \rangle$ in two adjacent cells divided by d with $\nabla_z \langle n \rangle$ one finds from Eq. [3.10]

$$\langle j_z \rangle = -D_0 \frac{1}{1 - \phi} \times \frac{1 - 2\phi p_{1,0}/aG(4\pi/3)^{1/2}}{1 + \phi p_{1,0}/aG(4\pi/3)^{1/2}} \nabla_z \langle n \rangle. \quad [3.11]$$

Comparing this expression with Eq. [3.1] we find the expression for the effective self-diffusion coefficient

$$D_{\text{eff}}/D_0 = \frac{1}{1 - \phi} \frac{1 - 2\phi p_{1,0}/aG(4\pi/3)^{1/2}}{1 + \phi p_{1,0}/aG(4\pi/3)^{1/2}}. \quad [3.12]$$

The factor $(1 - \phi)$ in the denominator is the so-called tortuisity factor and is given by the volume fraction which is accessible for the diffusing molecules for the system under consideration. The importance of this factor was first pointed out by Bell (2) and is the origin of the difference between his result and the expression given by Wang (1).

4. THE CALCULATION OF THE EFFECTIVE SELF-DIFFUSION COEFFICIENT

In order to find the behavior of the effective self-diffusion coefficient as a function of the volume fraction of the colloidal particles we have to solve the dipole moment $p_{1,0}$ from the infinite set of linear equations [2.8]. An analytic solution which is exact up to a certain power in the volume fraction may be obtained by solving Eq. [2.8] iteratively. In proceeding this way Eq. [3.10] can be written as

$$D_{\text{eff}} = D_0 \frac{1}{(1 - \phi)} \frac{(1 - 2K\phi)}{(1 + K\phi)}, \quad [4.1]$$

where $K = \sum_i m_i(\phi/\phi_{\max})^{i/3}$. With $(\phi/\phi_{\max})^{1/3} = (2a/d)^3$ and $\phi_{\max}$ is the volume fraction of the spheres at dense packing, these volume fractions for the cubic arrays are

$$\phi_{\max} = \pi/6 \cong 0.524, \quad \text{SC}$$
$$\phi_{\max} = (\pi/8)\sqrt{3} \cong 0.680, \quad \text{BCC}$$
$$\phi_{\max} = (\pi/6)\sqrt{2} \cong 0.741, \quad \text{FCC} \quad [4.2]$$

The first eight nonvanishing coefficients m_i are

$$m_0 = 1/2$$
$$m_{10} = (3)2^{-10} U_{4,0}^2$$
$$m_{14} = \left(\frac{55}{3}\right) 2^{-13} U_{6,0}^2$$

$$m_{17} = -(45)2^{-17}U_{4,0}^2 U_{6,0}$$

$$m_{18} = \left(\frac{35}{33}\right)2^{-14}U_{8,0}^2$$

$$m_{21} = -\left(\frac{35}{3}\right)2^{-17}U_{4,0}U_{6,0}U_{8,0}$$

$$m_{22} = \left(\frac{171}{65}\right)2^{-17}U_{10,0}^2$$

$$m_{24} = (675)2^{-24}U_{4,0}^2 U_{6,0}^2. \qquad [4.3]$$

We furthermore made use of the relation (13) $U_{l,m} : U_{l,0} = c_{l,m} : c_{l,0}$ to express lattice sums with $m \neq 0$ in terms of lattice sums with $m = 0$. Here $c_{l,m}$ denotes the coefficient of $Y_{l,m}$ in the expression for the completely symmetric cubic harmonic of order l which also may be found in Ref. (13). The lattice sums up to $l = 10$ are given in Table I for the three cubic arrays, i.e., the simple cubic (SC), the body centered cubic (BCC), and the face centered cubic (FCC).

When we expand the expression [4.1] for the effective self-diffusion coefficient D_{eff}/D_0 in a series of positive powers of $\phi^{1/3}$ we find

$$D_{\text{eff}}/D_0 = 1 - 0.5\phi + 0.25\phi^2 - 0.125\phi^3 + 0.0625\phi^4 + O(\phi^{13/3}). \qquad [4.4]$$

The first two terms on the right-hand side were first given by Bell (2). When we expand the result $D_{\text{eff}}/D_0 = (1 + 0.5\phi)^{-1}$ of Ref. (3) in positive powers of ϕ we find that this expression coincides with the series of Eq. (4.4) up to order ϕ^4. The next term in our expansion is of the order $\phi^{13/3}$ and is not of the order ϕ^5, as found when one expands the result in Ref. (3). Note that the coefficients of the terms of order $\phi^{13/3}$ and higher, contrary to the coefficients of the lower-order terms, depend explicitly on the type of array in which the spheres are placed. It follows that for volume fractions which are not too large the effective self diffusion coefficient is independent of the lattice type. It is to be expected that Eq. [4.4] may also be used for random arrangements of spheres, provided the volume fraction is sufficiently small.

TABLE I

The Values of the Lattice Sums $U_{l,0}$ for $l \leq 10$ for the Three Cubic Lattices

	SC	BCC	FCC
$U_{4,0}$	3.1083	−1.513	−1.331
$U_{6,0}$	0.5698	1.989	−2.374
$U_{8,0}$	3.2713	2.099	3.59
$U_{10,0}$	1.0096	−1.931	−0.043

The iterative method and the resulting exact coefficients in the expansion of D_{eff} in the cube root of the volume fraction are found to converge poorly for $\phi > 0.85\phi_{\max}$. Similar convergence problems occurred in the calculation of the effective rate coefficients studied in Ref. (6). As in that case, this problem is overcome if one uses the method of direct inversion. In this method one inverts the linear set of equations (cf. Eq. [2.8]) for the multipole moments $p_{l,m}$ exactly for a given number of multipoles as a function of the volume fraction. The advantage of this method is that, up to the order of multipoles considered, all interactions between these multipoles are taken into account, which is not the case with the iterative method. From this we calculate the effective self-diffusion coefficient, increasing the number of multipoles until the required convergence is obtained. At first we took only the $p_{1,0}$ into account. In subsequent steps we took all multipole moments $p_{l,m}$ with $l \leq 3$, $l \leq 5$, $l \leq 7$, $l \leq 9$, $l \leq 11$, $l \leq 13$, and $l \leq 15$, which gives 2, 5, 8, 13, 18, 25, and 32 multipole moments, respectively. Table II gives the resulting values of D_{eff}/D_0 at dense packing as a function of the number of multipoles taken into account. In Fig. 1 the curves of D_{eff}/D_0 as a function of the volume fraction obtained by the method of direct inversion are plotted for the three cubic lattices. For comparison we have also plotted the expression given in Ref. (3). A notable consequence of the contributions due to higher-order multipoles which differs from the behavior predicted by the formula given in Ref. (3) is that D_{eff} becomes a concave function of the volume fraction for volume frac-

TABLE II

The Value of D_{eff}/D_0 at the Volume Fraction of Dense Packing of the Spheres for the Cubic Lattices Obtained by the Method of Direct Inversion

M	SC	BCC	FCC
1	0.793	0.746	0.730
2	0.735	0.727	0.697
5	0.729	0.690	0.639
8	0.725	0.689	0.634
13	0.724	0.688	0.632
18	0.723	0.688	0.632
25	0.722	0.688	0.632
32	0.722	0.688	0.632

Note. M indicates the total number of multipoles included in the calculation.

tions larger than ca. 50% of the volume fraction at close packing.

5. EXPERIMENTAL PART

The behavior of the self-diffusion coefficient of the water molecules in latex suspensions has been measured by means of the 1-H NMR spin–echo pulsed field gradient method. In these measurements two different latices, polystyrene (PS) latex and polymethyl methacrylate methacrylic acid (PMMA) latex, were used. Both dispersions were salt-free and consisted of monodisperse, spherical latex particles, composed of entangled polymeric chains, in water. The spherical shape of the latex particles is stabilized in water by the hydrophobic effect. Owing to the dissociation in water of the built-in acid groups, the PS and PMMA latex particles are negatively charged.

Due to the long-range electrostatic interaction the latex particles organize themselves in an ordered structure, i.e., a colloidal crystal. This order is clearly indicated by the iridescence of the samples due to Bragg reflections. For both latices transmission measurements using thin latex films support the existence of the FCC arrangement (16). This long-range order of the samples enables a direct comparison to be made of the measurements with the theoretical predictions.

5.1. Preparation, Purification, and Characterization of the Latices

Monodisperse PMMA-latex was obtained from D.S.M. Resins B.V., The Netherlands (Product No.: ER20C3). The latex is synthesized by emulsion polymerization on the basis of methyl methacrylate/methacrylic acid (95/5) and sodium dodecylbenzenesulfate as emulsifier. From the suspension, residual monomers and other small molecules are removed as

(1) Dialysis against frequently refreshed, deionized, and Millipore filtered water, henceforth simply referred to as water. After ca. 120 h the dialysis is stopped, when the specific conductance in the water containing compartment has reached a constant value which is approximately equal to the pure water value of ca. 1×10^{-6} cm^{-1} Ω^{-1}.

(2) The latex is mixed with Amberlite MB-3 mixed bed ion-exchange resin and stored for 10 days, while being stirred frequently. The ion-exchange resin is removed by filtration through glass wool.

(3) To ensure removal of the monomer methyl methacrylate, the latex is heated at 60°C, while N_2 gas is bubbled through, until the specific smell of the monomer can no longer be detected.

(4) Final dialysis against water.

Spectrophotometrically (UV-spectroscopy with λ in the range of 240–330 nm), it is verified that the water phase, which is removed from the stock latex with the help of a centrifuge, does not contain any detectable amount of emulsifier. This means that the amount of emulsifier is smaller than 0.05 g/liter. Before use, the glassware and cellulose tubes (Visking; diam: 30 mm) are cleaned by heating them in an EDTA solution and in a $NaHCO_3$ solution. The cellulose tubes are stored in water. The ion-exchange resin and glass wool were rinsed thoroughly with water and were used directly afterwards.

The monodisperse polystyrene latex has been prepared in our laboratory by Dr. S. Sa-

saki (17). The latex is synthesized by emulsion polymerization of styrene and sodium styrenesulfonate with sodiumdodecylsulfate as emulsifier. The purification of the PS latex is similar to the one for the PMMA latex described above.

Some characterization properties of the PS and PMMA stock latex are given in Table III where the experimental details are described in notes A to P of this table.

5.2. *Preparation of the Concentration Series*

In order to obtain samples with different volume fractions of latex particles than the stock latices ($\phi \cong 0.1$), a concentration series of lattices is prepared from these stock latices by evaporation (to obtain suspensions with $\phi > 0.1$) or by dilution (to obtain suspensions with $\phi < 0.1$) with water. The evaporation of water is performed at room temperature, while N_2 gas is bubbled through the latex. For each of the latices obtained in this way the weight fraction S of the latex particles is determined. The volume fraction ϕ is calculated from the weight fraction S, using

$$\phi = \frac{\rho_w S}{\rho_l + (\rho_w - \rho_l)S}, \qquad [5.1]$$

where ρ_l and ρ_w denote respectively the density of the latex particles and that of pure water at temperature T. For PS and PMMA latex the values for ρ_l are given in Table III. The value for ρ_w is obtained from literature (18).

5.3. *Dynamic Light Scattering*

In order to avoid any possible confusion in this section, we first emphasize the fact that

TABLE III

	PMMA	Note	PS	Note
Weight fraction of latex particles	0.105	A	0.100	B
Density of the latex (g/cm^3)	1.210 ± 0.005	C	1.045	D
Glass transition temperature Tg (°C)	105	E	100	F
Effective hydrodynamic radius of latex particle (Å)	735 ± 42	G	669 ± 49	H
Number of latex particles/gram latex particles	5.0×10^{14}	I	7.6×10^{14}	J
Amount of acid groups/latex particle	2.5×10^4	K	2.1×10^4	L
Number of polymeric chains/latex particle	8244	M	244	N
Weight averaged molecular weight of chains; $\langle \overline{Mw} \rangle$ (g/mol)	147,000	O	3,230,000	P

Note. A, B: Weight fraction of latex is determined by drying to constant weight of a known amount of latex in vacuum at 40°C in the presence of P_2O_5. C: Derived from the measured densities of PMMA latices as a function of the weight fraction at 25°C. The densities were determined using a conventional pycnometer. The results agree well with the result for polymethylmethacrylate given in literature, i.e., 1.188 g/cm^3 at 25°C (20). D: Obtained from literature for 20°C (21). E, F: Obtained from literature (20). G, H: Determined by dynamic light scattering experiments. See text for details. I, J: Calculated with results denoted in this table. K: Obtained from conductometric titrations with NaOH in water. It is noted that the amount of acid groups is only ca. $\frac{1}{30}$ of the total amount one estimates from polymerization recepture. However, the latter amount is found experimentally by conductometric titration with NaOH in an aceton/water solution of PMMA latex which, before titration, has been dissolved in aceton. These observations suggest that not all of the acid groups reside on the surface of the latex particle. L: Obtained from conductometric titrations with NaOH in water. Solvation of PS latex in toluene and titration in a water/toluene solution leads to the same result. The titrations indicate that from the total amount ca. 70% are strong and 30% are weak acidic groups. M, N: Calculated with results denoted in this table. O: Derived from static light scattering experiments using Zimm's procedure (22). The experiments are performed on a Fica-50 photometer at 436 nmm and at 25°C. The refractive index increment of PMMA latex in methyl-ethylketone of 0.117 ± 0.001 ml/g is measured on a Brice-Phoenix refractometer at 436 nm and at 25°C. P: Similar to the procedure outlined in Note O with PS latex in toluene. For the refractive index increments of PS latex in toluene at 436 nm and at 25°C, the result 0.101 ± 0.001 ml/g is obtained.

all samples used in the dynamic light scattering experiment are obtained by diluting the concentration samples used in the NMR experiment described below, to a very low latex concentration. The dynamic light scattering experiments in the high-dilution limit are done in order to obtain information about the effective hydrodynamic radius of the latex spheres. Furthermore, the volume fraction ϕ in this section indicates the volume fraction of the latex from which the sample used in the dynamic light scattering experiment is obtained by dilution, rather than the volume fraction of the sample itself.

The dynamic light scattering experiments utilize an ALV-3030 digital correlator and a photomultiplier. The light source is a Spectra-physics 2020 argon ion laser, operating at 514.5 nm with 2.5 W maximum output. The intensity time correlation function is obtained by using 96 channels with a sample time of 20 μs. With the salt-free PS and PMMA latices very dilute samples are prepared. To avoid multiple scattering care is taken that for each sample studied the countrate of the photons does not exceed ca. 300 kHz. The samples are measured after filtration through 0.65-μm Fluoropore filters (Millipore). For each of the measured correlation functions the average sample temperature is registered. All experiments are performed at 25°C. To minimize the influence of dust on the time correlation function, a dust discrimination method is applied in which the output data from the correlator is rejected if the total number of photons detected during a time period of 30 s surpasses a threshold value. All the correlation functions are obtained with the scattering angle of 90°. The experimental correlation functions are analyzed by means of the following cumulant expansion:

$$g_1(t) = C \exp\left[-K_1 t + \frac{K_2}{K_1^2}(K_1 t)^2 - \frac{K_3}{3K_1^3}(K_1 t)^3 + \cdots\right] + B, \quad [5.2]$$

where K_i is the ith cumulant, C is a factor depending on the experimental conditions, and B is the baseline, which, as in ideal cases, is taken equal to one. K_1 is related to the self-diffusion coefficient D of a latex particle and the scattering vector $\mathbf{q}$, as

$$K_1 = 2D|\mathbf{q}|^2. \quad [5.3]$$

It is observed that the value of D does not depend on the scattering vector $\mathbf{q}$ in the range of 30–150°. For fitting the time correlation function a second-order cumulant expansion is used. In all measurements the value of the reduced second-order cumulant moment is moderate (i.e., $K_2/2K_1^2 \leq 0.1$), indicating that the effects of polydispersity of the latex spheres may be neglected. The effective hydrodynamic radius of the latex particle R_H^{eff} is calculated using the Stokes–Einstein relation:

$$R_H^{eff} = \frac{kT}{6\pi\eta D}, \quad [5.4]$$

where k is Boltzmann's constant and T is the absolute temperature. For the viscosity η the value at temperature T is linearily interpolated with the help of the literature data of pure water (18).

In Table IV and Fig. 2 the results for the effective hydrodynamic radius R_H^{eff} for the latex particles for the PS and PMMA latices are given, with ϕ indicating the volume fraction of the latex spheres (obtained from the weight fraction S and Eq. [5.1]) from which the sample is prepared by dilution. The average values and standard deviations are calculated with at least 20 different correlation function determinations per sample. It is observed that the effective hydrodynamic radii do not change with time; i.e., consistent results are obtained with recently purified latices and latices which, after purification, have been stored for one and a half years in a dark room at 4°C. The origin of the increase of the effective hydrodynamic radii as a function of ϕ, cf. Fig. 2, will be further investigated. Figure 2 shows that this effect is more pronounced for PMMA latex than for PS latex. With a nonweighted linear least-square fit the volume fraction dependency of R_H^{eff} is given by

$$R_H^{eff}(\phi) = (718 \pm 9) + (326 \pm 35)\phi$$

in Å for PMMA

$$R_H^{eff}(\phi) = (649 \pm 7) + (161 \pm 25)\phi$$

in Å for PS, [5.5]

with R_H^{eff} indicating the effective hydrodynamic radius and ϕ indicating the volume fraction of the latex from which the sample used in the dynamic light scattering is obtained by dilution.

5.4. NMR Measurements

The effective self-diffusion coefficient D_{eff} of the water molecules in the latices as a function of the volume fraction of latex particles is determined by means of the 1-H NMR pulsed field gradient technique with a steady background gradient. All measurements are performed at 25.0°C on a homebuilt spectrometer equipped with a 2.1 T electromagnet. For a description of the pulsed field gradient method we refer to Ref. (19). The measurements of the effective self-diffusion coefficient D_{eff} of the water molecules are based on a calibration using pure water as a reference with a value of $D_0 = 2.30 \times 10^{-9}$ m^2 s^{-1} at 25.0°C. The effective diffusion time between the gradient pulses is 6 ms. The results for the effective self-diffusion coefficient D_{eff} of the water molecules scaled by the value for pure water D_0 as a function of the volume fraction of the latex particles are given in Table V. It appears that

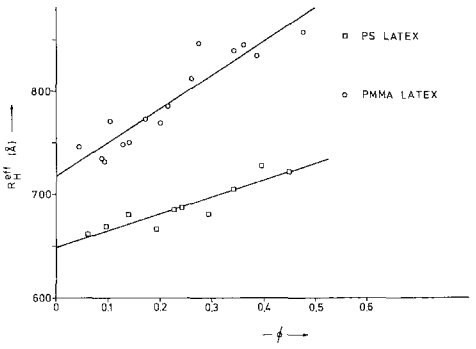

FIG. 2. The effective hydrodynamic radius R_H^{eff} as a function of the volume fraction ϕ of the latex, as obtained from the weight fraction S and Eq. [5.1], from which the sample used in the dynamic light scattering experiment is obtained by dilution. The measured points for the PS latex are denoted by (□) and for PMMA latex by (○). The solid curves are obtained from Eq. [5.5].

TABLE IV

The Effective Hydrodynamic Radius R_H^{eff} for the PS and PMMA Lattices as a Function of ϕ, as Determined by the Weight Fraction S and Eq. [5.1], of the Lattice from Which the Sample is Prepared by Infinite Dilution

PMMA		PS	
ϕ	R_H^{eff} (Å)	ϕ	R_H^{eff} (Å)
0.0441	746 ± 31	0.061	661 ± 67
0.0881	735 ± 42	0.096	669 ± 44
0.0929	732 ± 10	0.138	680 ± 49
0.104	771 ± 17	0.193	666 ± 38
0.128	748 ± 63	0.217	685 ± 20
0.140	750 ± 26	0.242	687 ± 53
0.171	773 ± 63	0.293	681 ± 62
0.199	769 ± 98	0.342	704 ± 38
0.215	785 ± 50	0.396	727 ± 82
0.260	812 ± 54	0.449	721 ± 38
0.275	846 ± 104		
0.343	839 ± 22		
0.362	845 ± 18		
0.388	834 ± 17		
0.480	857 ± 48		

TABLE V

The Value of the Effective Selfdiffusion Coefficient D_{eff}/D_0 of the Water Molecules in the PS and PMMA Lattices as Measured by the Pulsed Field Gradient NMR-Method as a Function of the Volume Fraction ϕ as Determined by the Weight Fraction S and Eq. [5.1]

PMMA		PS	
ϕ	D_{eff}/D_0	ϕ	D_{eff}/D_0
0.041	0.980	0.061	0.970
0.085	0.959	0.096	0.953
0.123	0.934	0.138	0.924
0.165	0.859	0.193	0.890
0.207	0.888	0.242	0.856
0.246	0.854	0.293	0.837
0.293	0.828	0.342	0.819
0.337	0.777	0.396	0.784
0.396	0.701	0.449	0.769
0.432	0.634		

the effective self-diffusion coefficients do not change in time, i.e., the results can be reproduced (within 3%) with samples that are stored for one and a half years in a dark room at 4°C.

6. COMPARISON WITH THEORY

In Fig. 3 the experimentally determined values for D_{eff}/D_0 are plotted as a function of the volume fraction ϕ together with the theoretical curve for the FCC lattice. It is noticed that the curves for the PS and PMMA latex coincide with each other only for volume fraction $\phi < 0.3$. Beyond $\phi \cong 0.3$ the curve for the PMMA latex falls below the curve for the PS latex. The theoretical value overestimates the value of the measured effective self-diffusion coefficient for all but the lowest volume fractions for both latices. This was also noted in Ref. (3) for the case of PMMA latex. The qualitative behavior of the theoretical curve is very similar to the experimental behavior, particularly for the PMMA latex. In the theoretical analysis the mobility of the water molecules is assumed to jump from the bulk value to zero on the surface of the latex spheres. Furthermore, in the calculation of the volume fraction of immobilized material these spheres are assumed to consist solely of polymer. In a more realistic description some of the water may also be immobilized either by swelling, or by hydration, or by both. It would then be more appropriate to plot the diffusion coefficient as a function of the total amount of immobilized material. This suggests that it is necessary to introduce an effective radius of the spheres which includes the immobilized water in addition to the latex. This situation is somewhat similar to the one encountered in the determination of the effective hydrodynamic radius of the latex particles through dynamic light scattering. The mobility of a latex sphere is also reduced by material which is immobilized with respect to the sphere. The light scattering data show a dependency of the effective hydrodynamic radius $R_{\text{H}}^{\text{eff}}$ of the latex particles on the volume fraction ϕ of latex; i.e., the volume fraction before the sample is diluted in order to do the dynamic light scattering experiment. The origin of this dependency is not clearly understood. Figure 3 suggests that a similar dependency on ϕ of the effective radius of the latex spheres in the NMR measurements of the self-diffusion coefficient of the water molecules might reconcile theory and experiment. To analyze how such a dependency affects the data we introduce the effective volume fraction

$$\phi_{\text{eff}} = \left[\frac{R_{\text{H}}^{\text{eff}}(\phi)}{R_{\text{H}}^{\text{eff}}(\phi = 0)}\right]^3 \phi. \qquad [5.6]$$

Of course this definition contains two rather ad hoc assumptions. The first is that for small volume fractions ϕ_{eff} becomes equal to ϕ. The second is that we may use the light scattering results to calculate the ϕ dependence of the effective radius. In Fig. 4 the experimental values for the effective self-diffusion coefficient are plotted as a function of the thus defined effective volume fraction ϕ_{eff} of the latex spheres. With the data plotted in this way we find that the experimental values for both latices follow the universal theoretical curve. At present further experiments are performed in order to clarify, on the one hand, the dependency of the effective hydrodynamic radius on the volume fraction of the latex, found using dynamic light scattering and, on the other, the

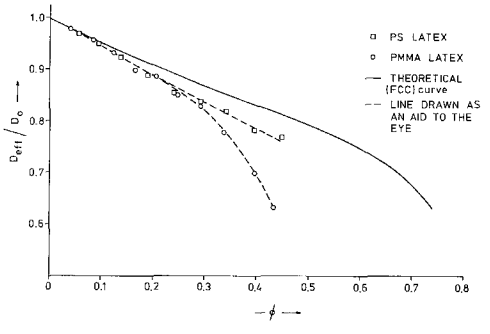

FIG. 3. The experimentally determined values for the scaled effective self-diffusion coefficient D_{eff}/D_0 as a function of the volume fraction ϕ, as obtained from the weight fraction S and Eq. [5.1]. The measured points are for the PS latex denoted by (□) and for the PMMA latex by (○). The solid curve denotes the theoretical result obtained by the method of direct inversion for the FCC array. The curves denoted by (---) are drawn as an aid to the eye.

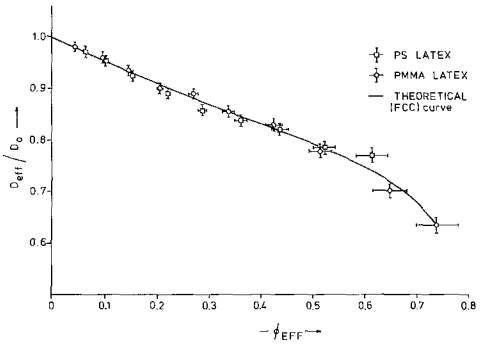

FIG. 4. The experimentally determined values for the scaled effective self-diffusion coefficient D_{eff}/D_0 as a function of the effective volume fraction ϕ_{eff}, as explained in the text. The measured points are for the PS latex denoted by (□) and for the PMMA latex denoted by (○). The solid curve denotes the theoretical result obtained by the method of direct inversion for the FCC array. The error bars in Fig. 4 denote a relative error of 1% in D_{eff}/D_0 and an error in ϕ_{eff} as estimated using Eqs. [5.5] and [5.6], using the laws of error propagation.

question of why the use of this radius in the theoretical expression for the effective self-diffusion coefficient of the water molecules yields agreement with the experimental results.

APPENDIX A

In order to write Eq. [2.5] in a more convenient form to analyze, we use the following expression (10, 14, 15), which enables us to expand the multipole fields originating from a sphere centered in $\mathbf{R}_1$ in terms of multipole fields originating from a sphere centered in $\mathbf{R}_2$:

$$\frac{1}{r_2^{l_2+1}} Y_{l_2,m_2}(\theta_2, \phi_2) = \sum_{l_1,m_1} H'(l_1 m_1 | l_2 m_2) \frac{Y_{l,m}(\theta_R, \phi_R)}{R^{l+1}} \times r_1^{l_1} Y_{l_1,m_1}(\theta_1, \phi_1), \quad [A.1]$$

with $l = l_1 + l_2$, $m = m_2 - m_1$.

Expression [A.1] is valid for $r_1 < R$. The vector $\mathbf{r}$ is the field point and $\mathbf{r}_1$ and $\mathbf{r}_2$ are defined by $\mathbf{r}_1 = \mathbf{r} - \mathbf{R}_1$ and $\mathbf{r}_2 = \mathbf{r} - \mathbf{R}_2$. We also define $\mathbf{R} = \mathbf{R}_1 - \mathbf{R}_2$. The spherical coordinates with angles measured relative to the fixed system are $\mathbf{r}_1 = (r_1, \theta_1, \phi_1)$ and $\mathbf{r}_2 = (r_2, \theta_2, \phi_2)$. The coefficients $H'(l_1 m_1 | l_2 m_2)$ are given by

$$H'(l_1 m_1 | l_2 m_2) = \sqrt{4\pi}(-1)^{l_2+m_1}\left[\frac{2l_2+1}{(2l_1+1)(2l+1)}\right]^{1/2} \times \left[\frac{(l+m)!(l-m)!}{(l_1+m_1)!(l_1-m_1)!(l_2+m_2)!(l_2-m_2)!}\right]^{1/2}, \quad [A.2]$$

with $l = l_1 + l_2$, $m = m_2 - m_1$.

ACKNOWLEDGMENT

This work was partly financed by the Dutch Paint Research Program (OSV).

REFERENCES

1. Wang, J. H., *J. Amer. Chem. Soc.* **76,** 4755 (1954).
2. Bell, G. M., *Trans. Faraday Soc.* **60,** 1752 (1964).
3. Jönsson, B., Wennerström, H., Nilsson, P. G., and Linse, P., *Colloid Polym. Sci.* **264,** 77 (1986).
4. Pieranski, P., *Contemp. Phys.* **24,** 25 (1983).
5. Monovoukas, Y., and Gast, A. P., *J. Colloid Interface Sci.* **128,** 533 (1989).
6. Venema, P., and Bedeaux, D., *Physica A* **156,** 835 (1989).
7. Jackson, J. D., "Classical Electrodynamics," 2nd ed., p. 99. Wiley, New York.
8. de Wette, F. W., and Nijboer, B. R. A., *Physica* **23,** 309 (1957).
9. McPhedran, R. C., and McKenzie, D. R., *Proc. R. Soc. London A* **359** 45 (1978).
10. McKenzie, D. R., McPhedran, R. C., and Derrick, G. H., *Proc. R. Soc. Lond. A* **362,** 211 (1978).
11. Hafkenscheid, L. M., Vlieger, J., *Physica* **75,** 57 (1974).
12. Lorentz, H. A., "Theory of Electrons," p. 137 ff. Dover, New York.
13. de Wette, F. W., *Physica* **25,** 1225 (1959).
14. Felderhof, B. U., *Physica A* **130A,** 34 (1985).
15. de Wette, F. W., and Nijboer, B. R. A., *Physica* **24,** 1105 (1958).
16. van Tent, A., and Struis, R. P. W. J., to be published.
17. Sasaki, S., *Colloid Polym. Sci.* **262,** 406 (1984).
18. "Handbook of Chemistry and Physics," 64th ed. CRC Press, Boca Raton, FL, 1983.
19. Hrovat, M. I., and Wade, C. G., *J. Magn. Reson.* **44,** 62 (1981).
20. "Polymer Handbook," (J. Brandrup and E. H. Immergut, Eds.), 2nd ed. Wiley, New York, 1975.
21. Hiltner, P. A., and Krieger, I. M., *J. Phys. Chem.* **73,** 2386 (1969).
22. Zimm, B. H., *J. Chem. Phys.* **16,** 1093 (1948).